Journal of Applied Sciences

ISSN 1812-5654

Journal of Applied Sciences 8 (18): 3068-3082, 2008
ISSN 1812-5654

Shear Modulus and Damping Ratio in Aggregate-Clay Mixtures: An Experimental Study Versus ANNs Prediction

A. Shafiee and R. Ghate
Geotechnical Engineering Research Center,
International Institute of Earthquake Engineering and Seismology, Tehran, Iran

Abstract: An extensive test program was conducted on kaolin-gravel and kaolin-sand mixtures to evaluate shear modulus, damping ratio and pore pressure of the mixtures. Test results reveal that shear modulus increases with aggregate content and confining stress and decreases with shear strain amplitude and loading cycles. Meanwhile, damping ratio depends mainly on aggregate content and shear strain amplitude and is less affected by loading cycles. Pore pressure also plays an important role in aggregate-kaolin mixtures and increases with aggregate content. An attempt has also been made to implement Artificial Neural Networks (ANNs) for modeling shear modulus, damping ratio and pore pressure build-up in the mixtures. The study indicates that ANNs can successfully model the complex relationship between cyclic deformation properties and input parameters including current state of stress, aggregate content, shear strain amplitude, confining stress, aggregate size and loading cycles.

Key words: Aggregate-clay, shear modulus, damping ratio, pore pressure, ANNs

INTRODUCTION

Compacted aggregate-clay mixtures are currently successfully used as the cores of embankment dams. These materials, called composite clays by Jafari and Shafiee (2004), are usually broadly graded and are composed of clay as the main body with sand, gravel, cobble or even boulders floating in the clay matrix. Karkheh and Gotvand dams in Iran are some recent examples of dams with cores composed of aggregate-clay mixtures.

It is also a current practice to employ the mixture of high plastic clay with aggregates as impervious blankets in waste disposal projects (Lee and Shackelford, 2005). It is generally assumed that the coarser fraction of such soils imparts a relatively higher shear strength and high compacted density while the permeability of the soil is governed by the proportion and index properties of the finer fraction (Shafiee, 2008).

Yin (1999) experimentally investigated the behavior of Hong Kong marine deposits with different clay contents. Test results revealed that the friction angle of deposits decreases with an increase in plasticity index. Young's modulus also increases with an increase in effective confining pressure but decreases with an increase in clay content. Vallejo and Mawby (2000) carried out a series of direct shear tests and porosity measurements on sand-clay mixtures. It was found that the percentage of sand in the mixtures had a marked influence on their shear strength. It was determined that when the concentration by weight of the sand in the mixtures was more than 75%, the shear strength of the mixtures was governed mainly by the frictional resistance between the sand grains. When the concentration of sand varied between 75 and 40%, the shear strength of the mixture was provided in part by the shear strength of the clay and in part by the frictional resistance between the sand grains. When the sand concentration was less than 40% by weight, the shear strength of the mixture was entirely dictated by strength of clay.

Muir Wood and Kumar (2000) conducted drained and undrained triaxial compression tests on isotropically normally consolidated and overconsolidated mixtures of kaolin clay and coarse uniform sand. It was found that the deviator stress, clay volumetric strain and pore pressure were unaffected by the presence of the sand until the clay content fell below 40%. Jafari and Shafiee (2004) carried out a series of strain-controlled monotonic and cyclic triaxial tests on gravel-kaolin and sand-kaolin mixtures to investigate the effects of aggregate on the mechanical behavior of the mixtures. Compression monotonic test results revealed that the angle of shearing resistance

Corresponding Author: A. Shafiee, Geotechnical Engineering Research Center,
International Institute of Earthquake Engineering and Seismology, No. 26, West Arghavan Ave., North Dibaji St., Farmanieh, Tehran, Iran Tel: +98 21 22281173 Fax: +98 21 22803656

increases with aggregate content. Prakasha and Chandrasekaran (2005) conducted an experimental study on reconstituted Indian marine soils having different proportions of sand and clay. Test results revealed that sand grains in clay leads to reduction in void ratio and increase in friction and pore pressure response resulting in decrease in undrained shear strength. Similarly, the inclusion of clay in sand leads to decrease in void ratio but imparts metastable character to the structure of sand and marks the sand behave in a manner consistent with a loose structure. All mixtures that fail during cycling considered in the study exhibit flow liquefaction and the soil with 90% sand content at low cyclic stress level exhibits limited liquefaction due to phase transformation.

A review of the published literature in monotonic loading reveals that, in general shear strength either increases with aggregate content or remains constant until a limiting aggregate content, then increases as the aggregate content increases. On the other hand, although expensive methods such as full scale and physical model tests can be conducted for evaluating behavior of composite clays with oversized particles, in many cases element tests are accomplished on materials of modified gradation. This modification in engineering projects can even be reduced to conduct tests only on pure clay by extracting the oversized particles. Published literature in monotonic loading clearly shows that the modification is a conservative estimation of the mechanical behavior of the mixture. However, Jafari and Shafiee (1998) showed that in the case of cyclic undrained loading on compacted aggregate-clay mixtures, the assumption that adding aggregate to pure clay improves its mechanical properties is questionable. They showed that the mixtures containing 50% sandy gravel and 50% high plastic clay, failed in a lower number of loading cycles and consequently exhibited less cyclic strength (defined as the ratio of deviator stress to initial confining stress causing 5% axial strain) than pure clays. Further comprehensive investigations by Jafari and Shafiee (2004) confirmed their previous study. It was concluded that when aggregate content is raised, excess pore pressure is also increased and consequently cyclic shear strength would decrease. This shows the need for understanding of different features of aggregate-clay mixtures behavior under cyclic undrained loading.

This research is composed of two parts: in the first part the cyclic deformation properties (i.e., shear modulus, damping ratio and pore pressure) of aggregate-clay mixtures tested previously by Jafari and Shafiee (2004) are thoroughly investigated and in the second part Artificial Neural Networks (ANNs) are used to examine the possibility of modeling the cyclic deformation properties of the heterogeneous materials.

MATERIALS AND METHODS

Materials tested: Pure clay with six mixtures of gravel-clay and sand-clay were used in this study. The physical properties of the materials were measured just prior to the beginning of the shear tests. Commercial kaolin clay was selected as the cohesive part. The kaolin had a specific gravity of 2.74 and its plasticity index was 38%. The X-ray diffraction analysis revealed that the clay was mainly composed of montmorillonite. The X-ray diffraction analysis was performed in the Iranian Geological Survey. The grain-size distribution curve for the clay is shown in Fig. 1. The aggregates that were mixed with the clay were retrieved from riverbed and composed of subrounded particles with a specific gravity of 2.66. Figure 1 shows the grain-size distribution curve of the parent granular material from which two types of aggregates, i.e., coarse sand and fine gravel were sieved. The aggregates passing through the 2.0 mm sieve and retained on the 1.68 mm sieve, with a minimum and maximum void ratio of 0.655 and 0.901, respectively, were used as the sand. The aggregates passing through the 6.35 mm sieve and retained on the 4.7 mm sieve with a minimum and maximum void ratio of 0.639 and 0.896, respectively were used as the gravel. The gap graded gradation was considered for the aggregates in order to focus on the impact of aggregate size on the mechanical behavior while minimizing the effect of particle size distribution.

Kaolin was mixed with respective amounts of sand and gravel to obtain various mixtures. The seven samples of aggregate-kaolin were mixed in volumetric proportion and named as K100, K80S, K80G, K60S, K60G, K40S and K40G, where the first letter is an abbreviation of Kaolin, the second number is the volumetric clay percent in the mixture and the third letter indicates the type of aggregate in the mixture (S stands for Sand and G for Gravel). A minimum of 40% clay content was considered since this is a limit value for materials used as cores in embankment dams.

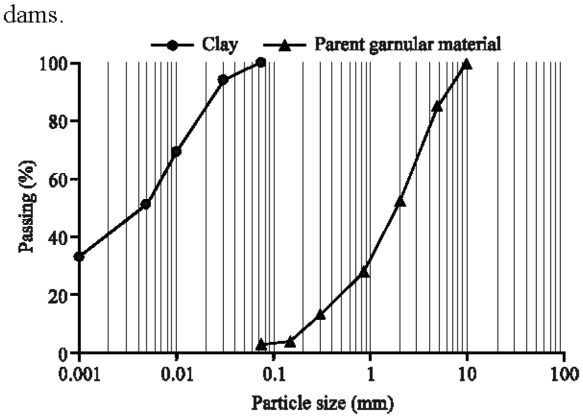

Fig. 1: Grain-size distribution for the soils used in the study

Specimen preparation: The specimen preparation technique was chosen in a manner to model as precisely as possible the *in situ* conditions of core materials of embankment dams. All the specimens, typically 50 mm in diameter and 100 mm in height were prepared, with a dry density of 95% of the maximum dry density obtained from the standard compaction test method and water content of 2% wet of optimum. Table 1 shows the specimens initial dry density and water content.

The appropriate amounts of kaolin and aggregate for each layer were first thoroughly mixed. Each layer was then mixed with water at least 24 h before use and sealed. The material was poured in 6 layers into a cylindrical mold and compacted. To achieve a greater uniformity of specimens, a procedure similar to undercompaction technique (Ladd, 1978) was used. For each layer, the compactive effort was increased towards the top by increasing the number of blows per layer. Each layer was then scored after it was compacted for better bonding with the next layer.

To reduce the effect of cap friction during the triaxial test, two thin rubber sheets coated with silicone grease were placed between the lower and upper porous stones and the specimen. Further, the sheets in contact with the specimen were divided into four sectors. This was done to let the specimen deform more easily in lateral directions. Five drainage holes with a diameter of about 5 mm were also provided in the rubber sheets to facilitate the saturation and consolidation process. The specimen preparation technique was verified when repeated testing of similar specimens yielded consistent results.

Test procedure: The specimens were saturated with a Skempton B-value in excess of 95%. To facilitate saturation process Carbon Dioxide (CO_2) was first percolated through the specimens (this was more effective for saturation of the low clay content specimens), then de-aired water flushed into the specimens. Finally a back pressure of 150 kPa was incrementally applied to accelerate the saturation rate. Then specimens were isotropically consolidated under three different effective confining stresses of 100, 300 and 500 kPa. Following consolidation, undrained cyclic triaxial tests were carried out under strain-controlled condition. Strain-controlled approach were also preferred over stress-controlled for cyclic loading tests, since previous researches strongly suggest that shear strain is a more fundamental parameter for studying pore pressure build-up than shear stress (Matasovic and Vucetic, 1992). The cyclic tests were continued until 50 cycles of loading as well. The loading rate shown in Table 2, was chosen so that pore pressure equalization through the specimen was ensured. The system used for conducting cyclic tests, was also an advanced automated triaxial testing apparatus.

Table 1: Specimens properties of initial dry density our water content

Specimen type	Initial dry density (g cm^{-3})	Initial water content (%)
K100	1.35	32.0
K80S, K80G	1.42	27.0
K60S, K60G	1.57	21.4
K40S, K40G	1.69	16.8

Table 2: Summary of testing program on each specimen

Confining stress (kPa)	Shear strain amplitude (%)	Loading frequency (Hz)
100	1.50	
	0.75	0.01
	0.15	
300	1.50	
	0.75	0.005
	0.15	
500	1.50	
	0.75	0.005

STRAIN DEPENDENT CYCLIC DEFORMATION PROPERTIES

Shear modulus and damping ratio are important soil properties that are used extensively in dynamic analyses. When cyclic triaxial tests are performed, a hysteresis loop will be formed by plotting the deviator stress, σ_d, versus axial strain, ε. The slope of the secant line connecting the extreme points on the hysteresis loop is the Young modulus, E, (Fig. 2) where:

$$E = \sigma_d/\varepsilon \tag{1}$$

As the axial strain amplitude increases, the Young modulus decreases, as shown in Fig. 2. Having obtained the values of E and ε, the shear modulus, G and shear strain, γ can be found through the following equations:

$$G = E/2(1+v) \tag{2}$$

and

$$\gamma = (1+v)\varepsilon \tag{3}$$

Where:

V = Poisson's ratio and may be estimated at 0.5 for saturated, undrained specimens

The damping ratio, D, is a measure of dissipated energy, W_D, versus elastic strain energy, W_S and may be computed with the Eq:

$$D = W_D/4\pi W_s \tag{4}$$

Referring to Fig. 2, the area inside the hysteresis loop is W_D and the shaded area of the triangle is W_S.

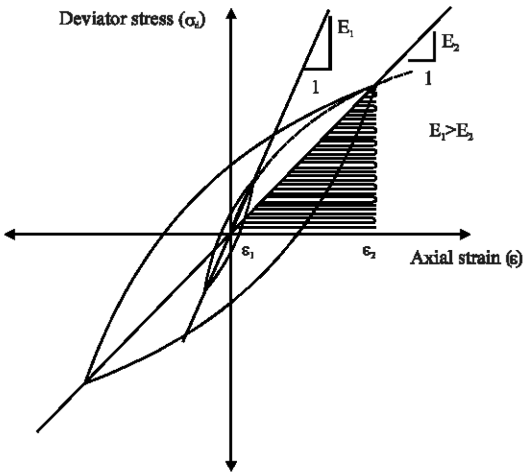

Fig. 2: Definition of strain dependent shear modulus and damping ratio in cyclic loading

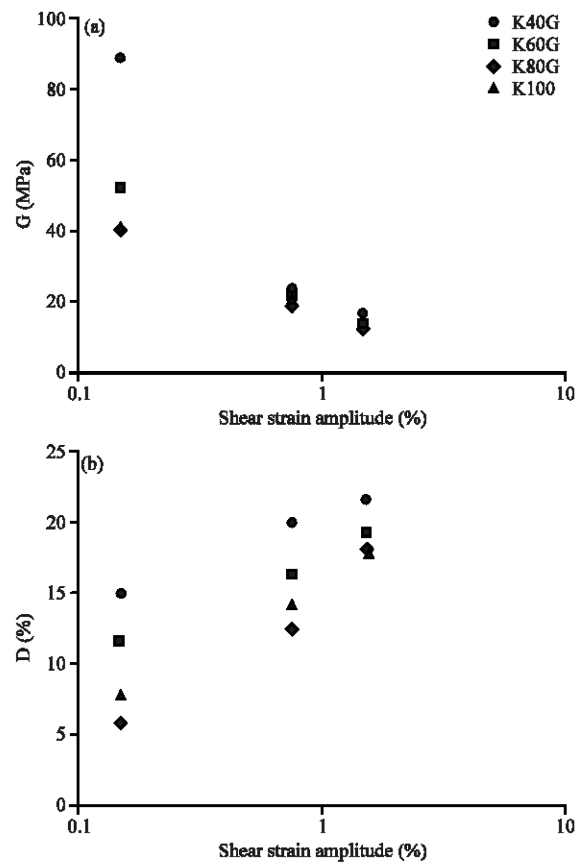

Fig. 3: Variation of (a) shear modulus and (b) damping ratio against shear strain amplitude in gravel-kaolin mixtures, $p'_0 = 100$ kPa and N = 2

The results are presented for the tests performed under an initial confining stress, p'_0 of 100 kPa and at 2nd loading cycle, N (the trend for other confining stresses

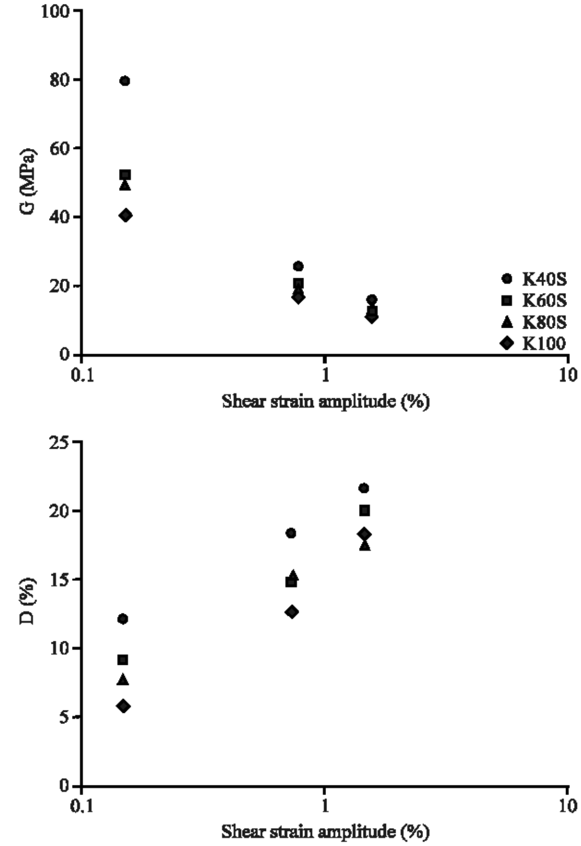

Fig. 4: Variation of (a) shear modulus and (b) damping ratio against shear strain amplitude in sand-kaolin mixtures, $p'_0 = 100$ kPa and N = 2

and cycles is the same and not shown herein). As can be seen in Fig. 3 and 4, for all mixtures, when shear strain amplitude increases, the shear modulus decreases and damping ratio increases. In addition, when aggregate content is raised both shear modulus and damping ratio increase. However, the effect of aggregate content on shear modulus diminishes at high shear strain amplitudes of order 1.5%. Thus, in general, K40G and K40S specimens exhibit the highest values of shear modulus and damping ratio, whilst the pure clay (i.e., K100) specimens exhibit the lowest ones.

DEPENDENCE OF SHEAR MODULUS ON AGGREGATE CONTENT AND LOADING CYCLES

Herein, the variations in shear modulus are presented for different shear strain amplitudes, γ_c under an initial confining stress of 100 kPa (the trend under other confining stresses is the same and not shown herein). As

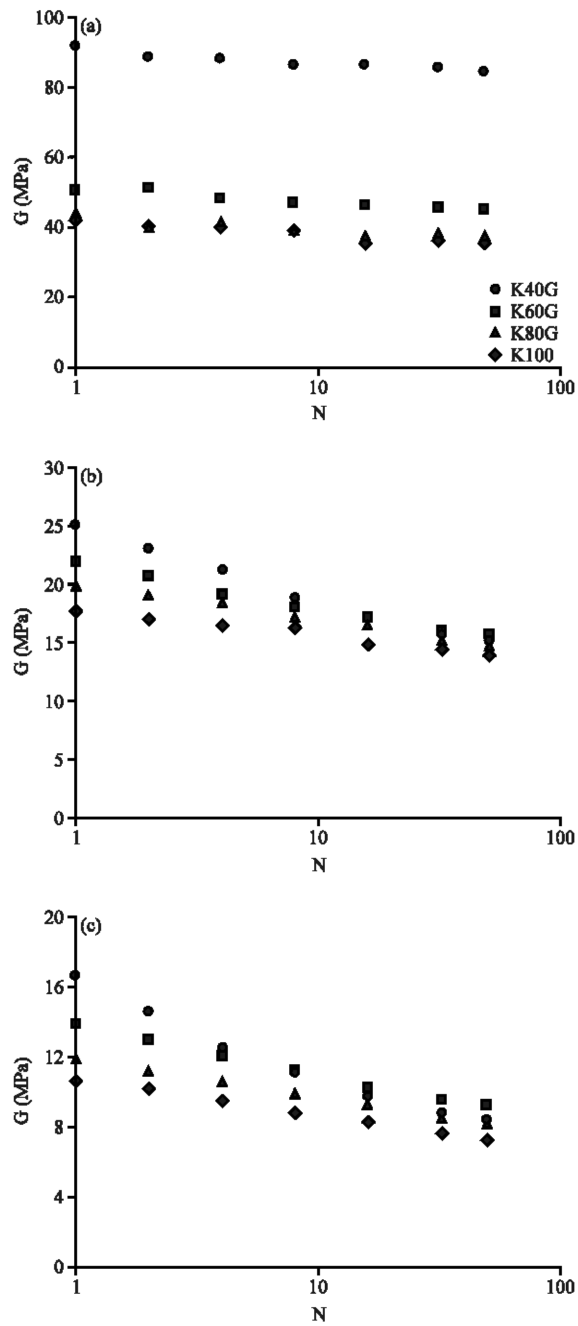

Fig. 5: Dependence of shear modulus on loading cycles in gravel-kaolin mixtures under $p'_0 = 100$ kPa (a) $\gamma_c = 0.15\%$ (b) $\gamma_c = 0.75\%$ and (c) $\gamma_c = 1.5\%$

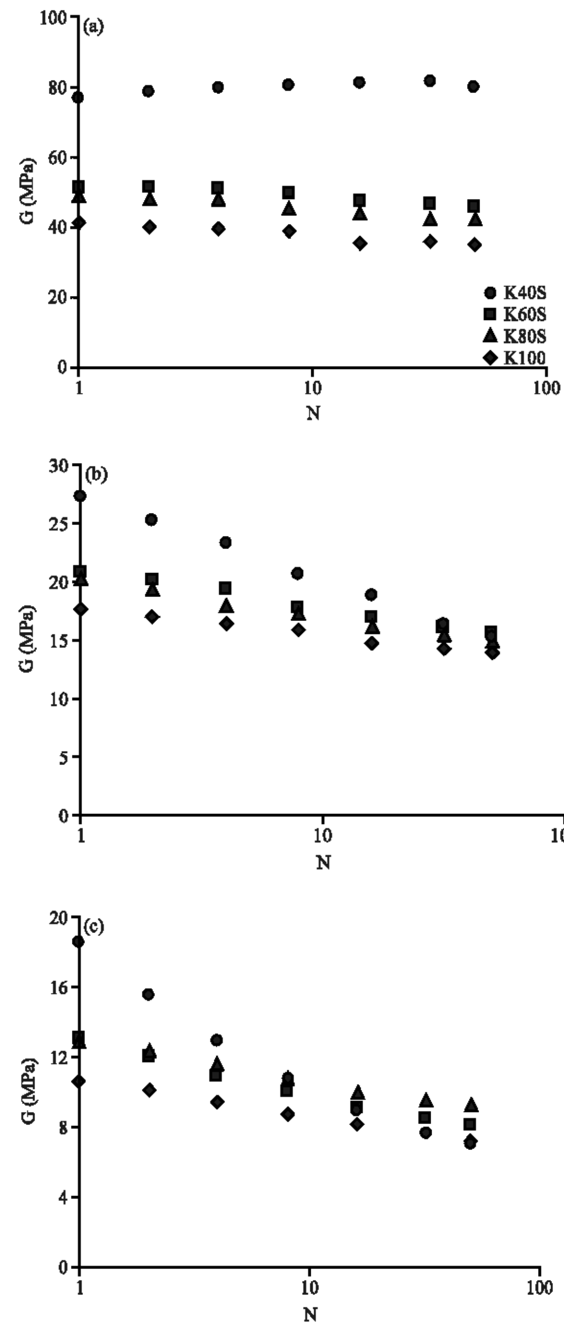

Fig. 6: Dependence of shear modulus on loading cycles in sand-kaolin mixtures under $p'_0 = 100$ kPa (a) $\gamma_c = 0.15\%$ (b) $\gamma_c = 0.75\%$ and (c) $\gamma_c = 1.5\%$

shown in Fig. 5a and 6a, under a low shear strain amplitude of 0.15%, in all mixtures shear modulus is independent of loading cycles and increases when aggregate content is raised. When the shear strain amplitude is increased to 0.75 or 1.5%, the behavior is quite different. As shown in Fig. 5b, c and 6c, under high shear strain amplitudes, shear modulus depends on loading cycles and decreases when loading proceeds. As can be seen, prior to 10th cycle of loading, shear modulus generally increases with aggregate content. After the cycle 10, shear modulus is nearly identical for all mixtures, because of severe decrease in shear modulus of

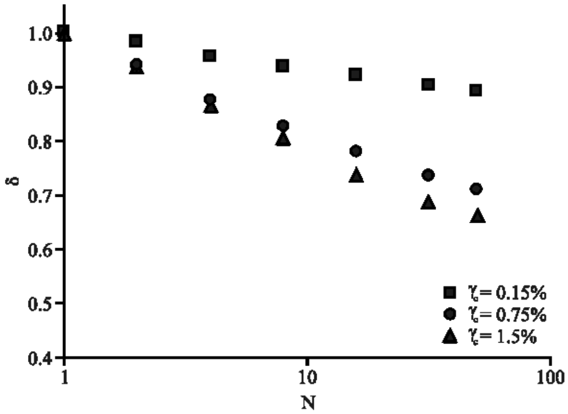

Fig. 7: Effect of loading cycles and shear strain amplitude on degradation index in specimen K60G, $p'_0 = 100$ kPa

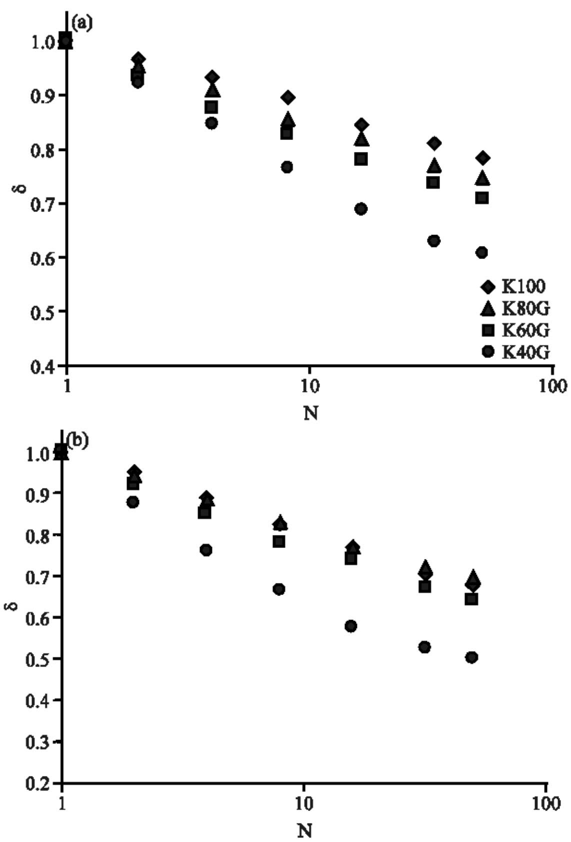

Fig. 8: Variation of degradation index in gravel-kaolin mixtures under $p'_0 = 100$ kPa (a) γ_c = 0.75% and (b) γ_c = 1.5%

specimens with high aggregate content. As will be explained later, the decrease in shear modulus is attributed to the pore pressure build-up when loading proceeds.

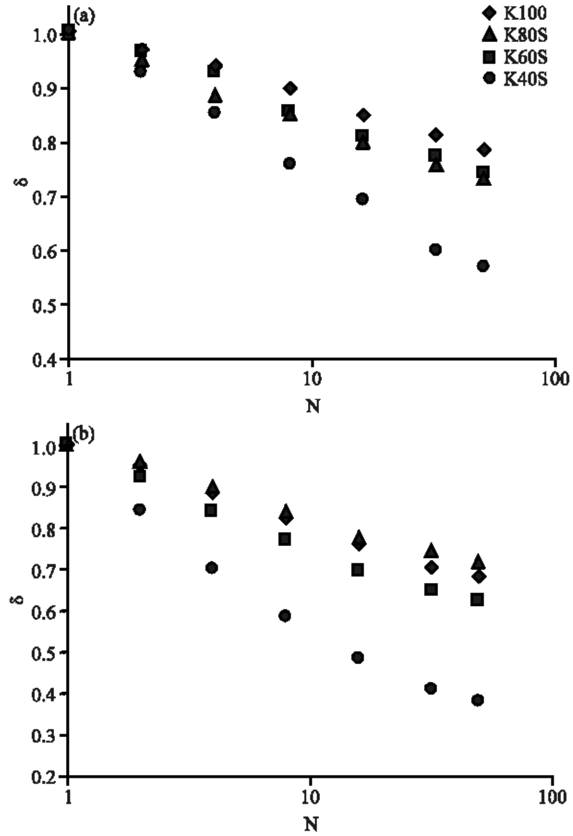

Fig. 9: Variation of degradation index in gravel-kaolin mixtures under $p'_0 = 100$ kPa (a) γ_c = 0.75% and (b) γ_c = 1.5%

To quantify the shear modulus dependence on cycles of loading and have more insight on the behavior, it is prudent to verify the variation of degradation index, δ (Idriss *et al*., 1978) in different mixtures. δ is defined as follows:

$$\delta = G_N/G_1 \qquad (5)$$

where, $G_1$and G_N denote the secant shear modulus in the first and Nth cycles of loading respectively. Figure 7 presents typically the variation of δ in terms of N for the specimens containing 40% gravel (i.e., K60G) for different shear strain amplitudes. The variation of δ in other mixtures obeys the similar trend shown for K60G specimens and hence it is not shown herein. As shown in Fig. 7, the value of δ depends on both cycles of loading and shear strain amplitude in such a manner that it decreases when these parameters increase.

The variation of δ with N, in gravel-kaolin and sand-kaolin mixtures, is shown in Fig. 8 and 9, respectively for shear strain amplitudes of 0.75 and 1.5%, under an initial confining stress of 100 kPa. As can be seen, in general, when aggregate content is raised, δ decreases. Hence, K100, K80G and K80S specimens have the highest values of δ, while K40G and K40S specimens have the lowest ones. The increase in degradation of shear modulus of high aggregate content mixtures may be attributed to the appreciable pore pressure build-up, as will be discussed later.

DEPENDENCE OF DAMPING RATIO ON AGGREGATE CONTENT AND LOADING CYCLES

As can be shown in Fig. 10 and 11, under a typical initial confining stress of 100 kPa, damping ratio increases with aggregate content. If enhancement in aggregate content is interpreted as decrease in plasticity, the observed trend is consistent with the curves of Vucetic and Dobry (1991) on the effect of soil plasticity on damping ratio. In addition, as shown in Fig. 10 and 11, damping ratio is almost independent of loading cycles. The reason can be readily explained. Figure 12, for example, presents the hysteresis loop formed in 2nd and 30th cycles of loading on specimen K80G under a shear strain amplitude of 0.75% and an initial confining stress of 500 kPa. As can be seen, the area of hysteresis loop (i.e., the dissipated energy) in the 30th cycle is less than that of 2nd cycle. However, the secant shear modulus in 30th cycle is less than 2nd cycle. In other words, in the 30th cycle the specimen absorbs less energy than 2nd cycle. It can be shown when loading proceeds the dissipated energy decreases with nearly the same order as absorbed energy decreases and hence according to Eq. 4, damping ratio does not change remarkably with loading cycles.

EFFECT OF AGGREGATE CONTENT ON PORE PRESSURE BUILD-UP

As indicated previously, the appreciable decrease in shear modulus of aggregate-clay mixtures may be attributed to the pore pressure build-up during cyclic loading. Figure 13 and 14 display the variation of u_N^* (which is pore pressure normalized to initial confining stress and computed where shear strain is zero) in terms of number of loading cycles, in gravel-kaolin and sand-kaolin mixtures respectively under shear strain amplitudes of 0.15, 0.75 and 1.5% and a typical confining stress of 100 kPa (the behavior under other confining stresses is the same and not shown herein). As seen, in general, pore pressure increases when aggregate content is raised. However, the trend is manifested when shear strain

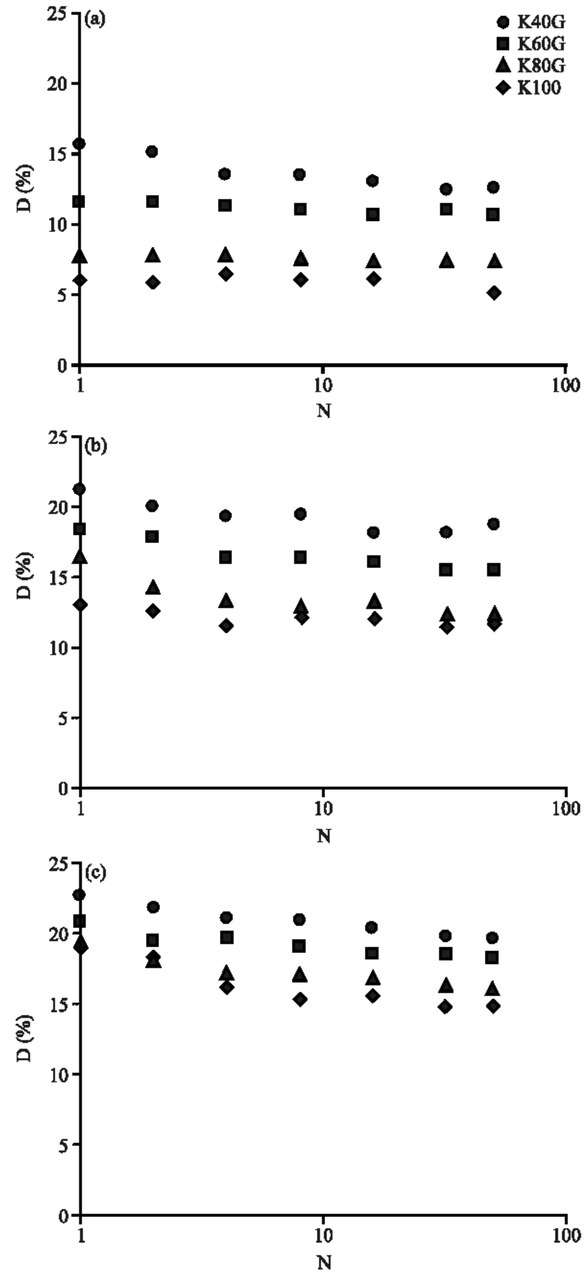

Fig. 10: Damping ratio in terms of loading cycles in gravel-kaolin mixtures under $p'_0 = 100$ kPa (a) $\gamma_c = 0.15\%$ (b) $\gamma_c = 0.75\%$ and (c) $\gamma_c = 1.5\%$

amplitude is increased. Thus u_N^* is highest for K40G and K40S specimens and lowest for K100 ones. As indicated by Jafari and Shafiee (2004), since the compressibility of clayey matrix is much more than individual grains, all of the specimen deformations take place in the clay. Hence, during a strain-controlled loading, the clayey matrix of specimens containing more aggregate experiences more

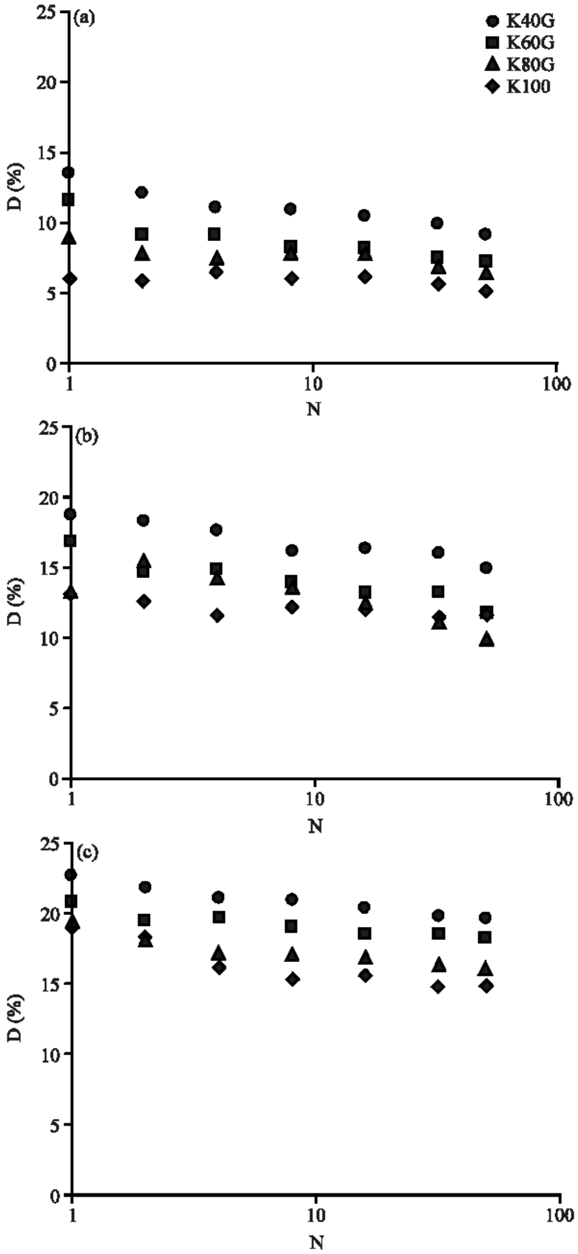

Fig. 11: Damping ratio in terms of loading cycles in sand-kaolin mixtures under $p'_0 = 100$ kPa (a) $\gamma_c = 0.15\%$ (b) $\gamma_c = 0.75\%$ and (c) $\gamma_c = 1.5\%$

deformation for the same strain level, directly leading to more pore pressure build-up. Jafari and Shafiee (2004) also reported that the heterogeneous field of effective stress and deformation developed in clayey matrix can be another reason for more pore pressure build-up in specimens containing more aggregates.

The trend of pore pressure variation shown in Fig. 13 and 14 is wholly consistent with the trend of degradation

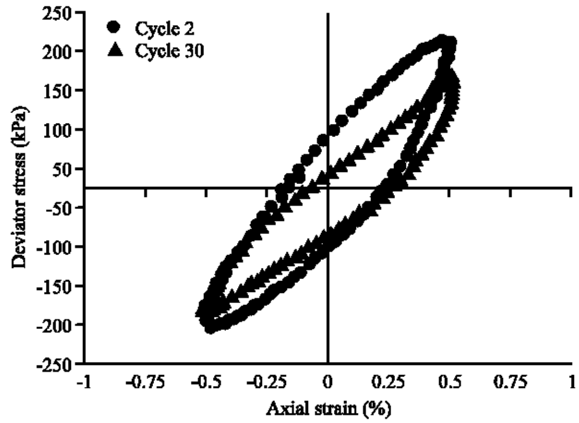

Fig. 12: Hysteresis loops for specimen K80G, $\gamma_c = 0.75\%$ and $p'_0 = 500$ kPa

index variation (Fig. 8 and 9). On the basis of the data presented in Fig. 13 and 14, it can be inferred that an increase in aggregate content would lead to decrease in effective confining stress when loading proceeds. Consequently, shear modulus would decrease more with loading cycles when aggregate content is raised.

EFFECT OF INITIAL CONFINING STRESS ON CYCLIC PROPERTIES

To explore the impact of confining stress on cyclic deformation properties, the tests were performed under various confining stresses of 100, 300 and 500 kPa. Figure 15a and b, for instance, presents the effect of initial confining stress on shear modulus in cycle 10, G_{10} under a typical shear strain amplitude of 0.75% in gravel-kaolin and sand-kaolin mixtures respectively. It is interesting to note that an increase in initial confining stress would increase shear modulus linearly. Figure 16a and b also present the variation of damping ratio in cycle 10, D_{10} under a shear strain amplitude of 0.75% in gravel-kaolin and sand-kaolin mixtures respectively. As can be seen, damping ratio is nearly unaffected by the initial confining stress.

EFFECT OF AGGREGATE SIZE ON CYCLIC PROPERTIES

One of the issues of concern in the experimental study was to assess the effect of aggregate size on the cyclic deformation properties. Hence, the tests were conducted on gravel-kaolin and sand-kaolin mixtures. The gravel and the sand had mean grain diameter of 5.55 and 1.84 mm, respectively. Figure 17, for instance, compares the impact of aggregate size on cyclic properties under an

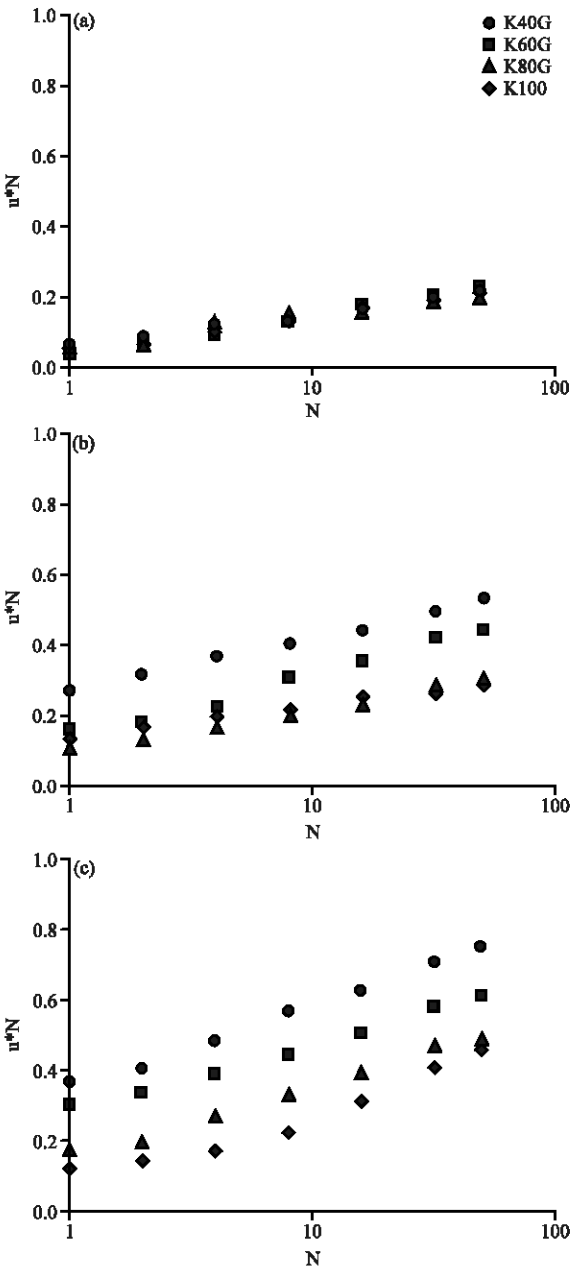

Fig. 13: Pore pressure build-up in gravel-kaolin mixtures under $p'_0 = 100$ kPa (a) $\gamma_c = 0.15\%$ (b) $\gamma_c = 0.75\%$ and (c) $\gamma_c = 1.5\%$

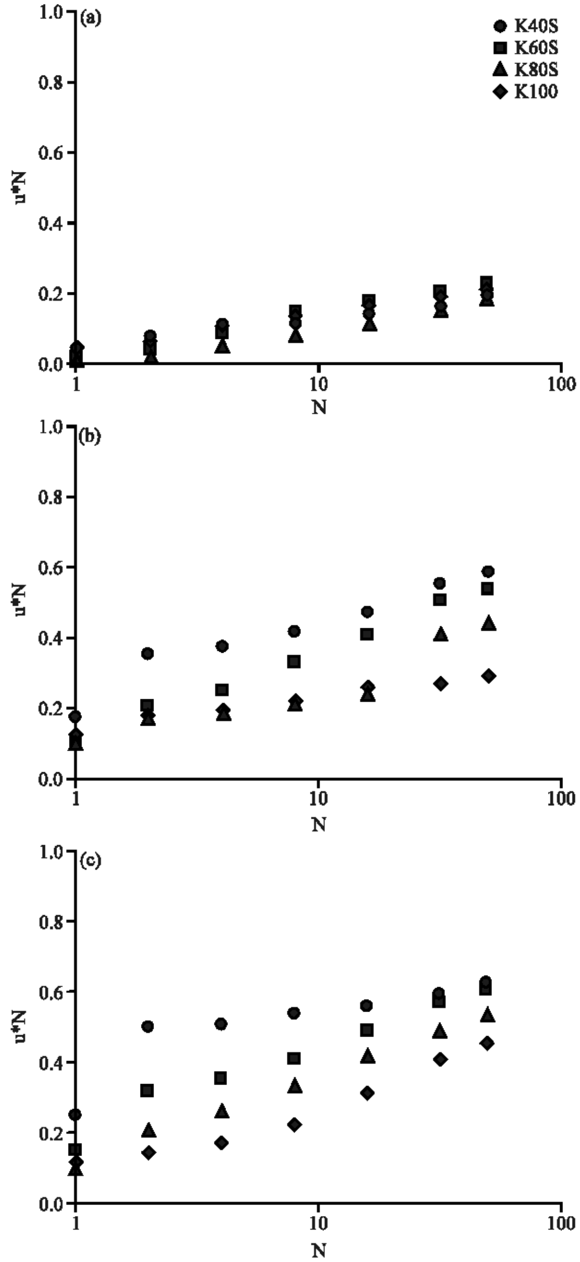

Fig. 14: Pore pressure build-up in sand-kaolin mixtures under $p'_0 = 100$ kPa (a) $\gamma_c = 0.15\%$ (b) $\gamma_c = 0.75\%$ and (c) $\gamma_c = 1.5\%$

initial confining stress of 100 kPa and a shear strain amplitude of 0.75%. As can be seen, aggregate size does not affect cyclic deformation properties markedly when aggregate content is low (i.e., 20%). In high aggregate content mixtures, particularly in mixtures containing 60% aggregates, shear modulus and pore pressure slightly decrease and damping ratio increases when aggregate size is increased.

ANNS MODELING OF SHEAR MODULUS, DAMPING RATIO AND PORE PRESSURE

Although accurate, it is often tedious and expensive to conduct laboratory tests on composite materials. One alternative to the lengthy laboratory determination of cyclic deformation properties can be the utilization of automated predictors that require only the input of easily

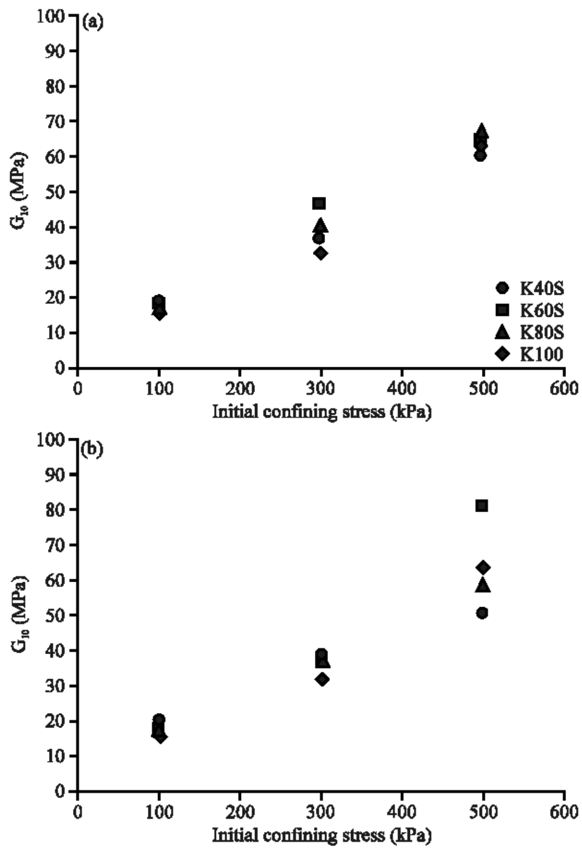

Fig. 15: Effect of initial confining stress on shear modulus in cycle 10 for (a) gravel-kaolin and (b) sand-kaolin mixtures under γ_c = 0.75% and $p'_0 = 100$ kPa

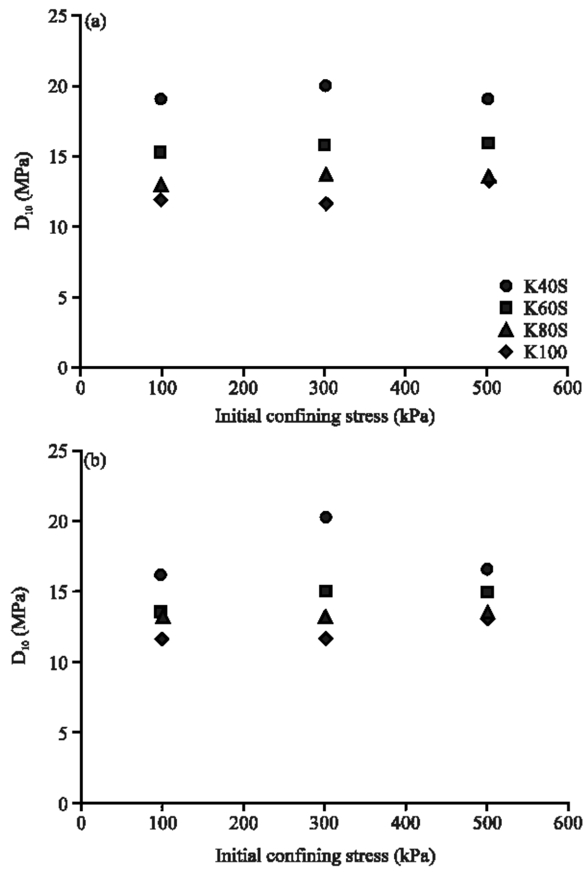

Fig. 16: Effect of initial confining stress on damping ratio in cycle 10 for (a) gravel-kaolin and (b) sand-kaolin mixtures under γ_c = 0.75% and $p'_0 = 100$ kPa

measurable parameters. Theses predictive methods can be utilized effectively for feasibility studies, early decision in the field, parametric analytical studies and such. Herein, Artificial Neural Networks (ANNs) are utilized to model the complex behavior of aggregate-clay mixtures.

Since a large body of ANN knowledge has been introduced in the literature, this issue is not addressed in detail herein. However, the salient features of this computational paradigm are explained. A neural network is a massively parallel distributed processor made up of simple processing units, which has a natural propensity for storing experiential knowledge and making it available for use. The procedure used to perform the learning process is called a learning algorithm, the function of which is to modify the synaptic weights of the network in an orderly fashion to attain a desired design objective (Haykin, 1999).

ANNs have been satisfactorily applied in the prediction of diverse problems in civil engineering. The advantage of ANNs is its capacity to learn complex functions between variables without the necessity of applying suppositions or restrictions a priori to the data. In recent years, the use of ANNs has increased in many geotechnical earthquake engineering issues and has demonstrated some degree of success. A review of the literature reveals that ANNs have been used successfully in evaluation of seismic site effects (Paolucci *et al*., 2000), prediction of maximum shear modulus and minimum damping ratio (Akbulut *et al*., 2004), assessment of earthquake-induced landslide (Lee and Envangelista, 2006) and assessment of liquefaction potential (Baziar and Jafarian, 2007).

In this study, the multilayer perceptron (MLP) was utilized to model the cyclic deformation properties. It is the most popular class of networks which has been applied to solve diverse civil engineering problems. A multilayer perceptron is composed of an input layer, an output layer and one or more hidden layers, however, it has been demonstrated that for the majority of problems only one hidden layer is enough. The architecture of a typical perceptron formed by an input layer, a hidden layer and an output layer is shown in Fig. 18.

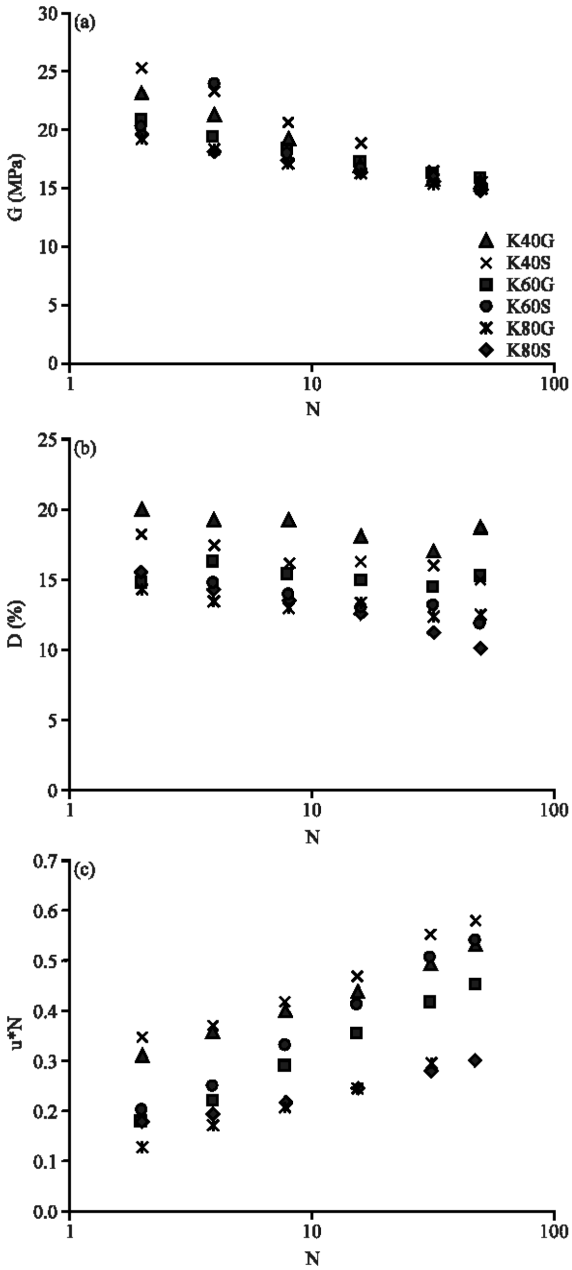

Fig. 17: Effect of aggregate size on (a) shear modulus (b) damping ratio and (C) pore pressure under $\gamma_c = 0.75\%$ and $p'_0 = 100$ kPa

Training, testing and validation datasets: The dataset used for training the networks is based on fifty six tests carried out on seven specimens namely K100, K80S, K80G, K60S, K60G, K40S and K40G (Table 2). It should be noted that by increasing the number of connection weights in networks, the networks can overfit the training data, particularly if the training data are noisy. In order to avoid overtraining, various rules are proposed to restrict the ratio of the number of connection weights to the number of data samples in the training set. Alternatively, the cross-validation technique can be used, in which the available data sets are partitioned into training, testing and validation subsets (Haykin, 1999).

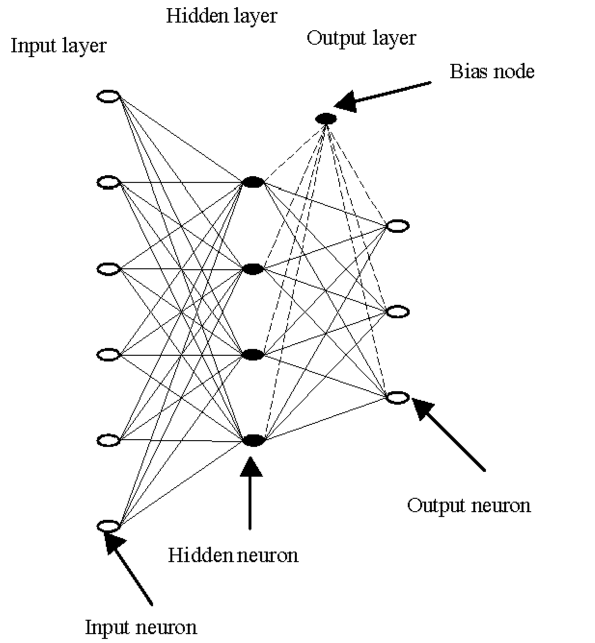

Fig. 18: The architecture of a typical perceptron

Table 3: Details of neural network models

Model	Predicted parameter	No. of hidden neurons	R	MSE
M1-G	Shear modulus	18	0.97	58.0
M1-D	Damping ratio	18	0.98	1.0
M1-U	Pore pressure	12	0.94	65.0
M2-(G,U)	Shear modulus	5	0.97	4.0
M2-(D,U)	Damping ratio	15	0.97	1.7
M2-U	Pore pressure	3	0.99	0.2

The training subset is used to adjust the connection weights, whereas the validation subset is used to check the performance of the network at various stages of learning. The test subset is also used for comparing the generalization of networks and selecting the best of them. In this study, data sets were randomly partitioned. Ten percent of the available data were used for testing, ten percent for validation and eighty percent of the remaining data were used for training. Subsequently, seven, seven and forty two tests were allotted to the test, validation and training subset, respectively.

The network architectures and input variables: The objective of training the neural networks was to predict the deformation properties of aggregate-clay mixtures under cyclic loading conditions. Two MLP models with different architectures were utilized. First model consists

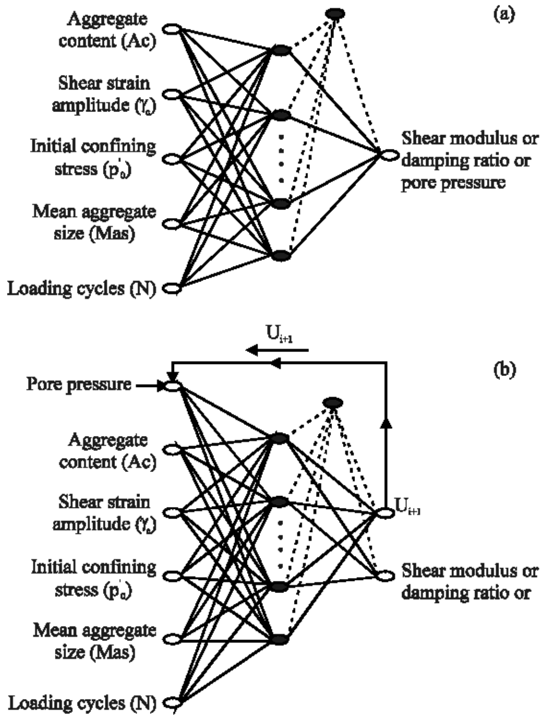

Fig. 19: The architecture of the proposed model for predicting the cyclic properties (a) M-1 and (b) M-2

of three layers: an input layer, a single hidden layer and an output layer (Fig. 19a). Henceforth this model is named M 1. The input parameters of M 1 are as follows:

- Aggregate content, Ac (%); the range of which is between 0 to 60.
- Shear strain amplitude, γ_c (%); which varies from 0.15 to 1.5.
- Initial confining stress, p_0' (kPa); the range of which is between 100 to 500.
- Mean aggregate size, Mas (mm); in the range of 0 to 5.55.
- Loading cycles, N; the range of which is between 0 to 50.

The output layer consists of a single neuron which predicts shear modulus (MPa), damping ratio (%) and pore pressure (kPa). Consequently, three networks M1-D, M1-G and M1-U predicting shear modulus, damping ratio and pore pressure, respectively, were trained.

Since the current state of stress affect the next state in the soils, a second model was constructed. It is similar to the first one in the sense that both of them have three layers. The main difference between the second model, namely M-2 and the first one (i.e., M-1) is that the model M-2, takes into consideration the current state of the stress by incorporating pore pressure (U_i) in Nth cycle of loading as an extra input which its value is equal to the output from network's forward computation of the last iteration. The model M-2 has two outputs: one is pore pressure in (N+1)th cycle of loading and the second is alternatively damping ratio or shear modulus (Fig. 19b). This type of network is also known as sequential network (McCelland and Rumelhart, 1988). As shown in Fig. 19b the predicted value of pore pressure in each step acts as the input value for the next step. Eventually, three networks namely M2-(D,U), M2-(G,U) and M2-U were trained, in the second model.

Training the network: Once the network weights and biases are initialized, the network is ready for training. During training the weights and biases of the network were iteratively adjusted to minimize the network performance function. The performance function used in the study was Mean Square Error (MSE), which is the average square error between the network outputs and the target outputs. The Levenberg-Marquardt was used as the training algorithm, since it has the fastest convergence (Haykin, 1999). The cross-validation technique was also utilized as the stopping criterion for training the networks. In this technique, as soon as MSE on the validation subset increases the training process stops. Whenever the iteration is stopped, MSE would be calculated for each of the training, testing and verification phases and compared.

Each of the 6 networks was trained using different number of hidden neurons and different activation functions. Next, the number of hidden neurons and the type of activation functions which produced minimum MSE and maximum correlation coefficient (R) were selected. Subsequently, the appropriate structure of each network was determined. Finally, the networks which best predicted the target values were selected. Table 3 presents the characteristics of the networks. On the basis of the values of MSE and R shown in Table 3, the first model predicts damping ratio better than the second one, while the second model performs better than the first model in predicting shear modulus and pore pressure. In other words, the current state of stress, which was considered by a feedback loop in the second model (Fig. 19b), plays an important role in determination of shear modulus and pore pressure while it is not an important parameter in predicting damping ratio. As previously indicated in Fig. 10 and 11, damping ratio is not affected by loading cycles, which is an indication of current state of stress.

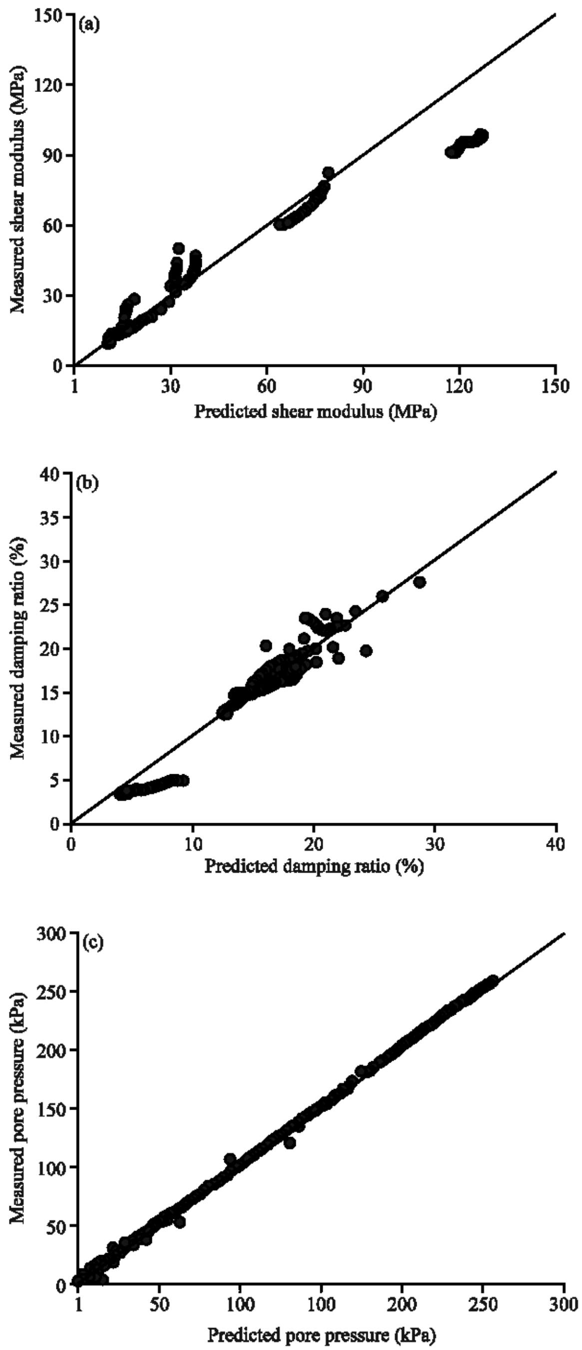

Fig. 20: Comparison of predicted cyclic properties and laboratory data (a) shear modulus (b) damping ratio and (c) pore pressure

The predictions using ANNs against laboratory data is plotted in Fig. 20. As can be seen, in spite of large values of shear modulus and low values of damping ratio, the ANNs appropriately predict the cyclic deformation properties.

Table 4: Relative importance (in percent) of input neurons

Model	Ac	γ_c	p'_0	Mas	N	U_i(current state of stress)
M2-(G,U)	27.9	24.1	14.3	1.80	3.00	29.0
M1-D	29.7	30.9	12.8	10.4	16.3	-
M2-U	31.3	7.30	24.7	1.30	15.6	19.7

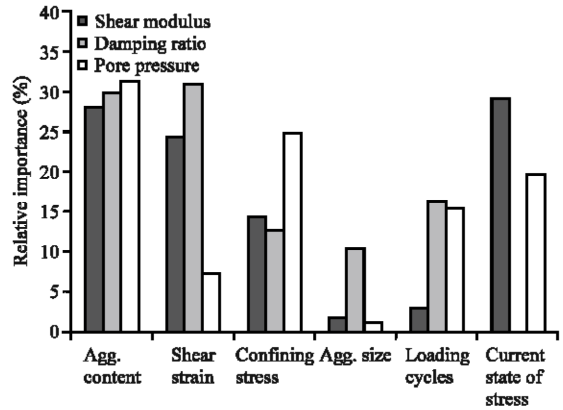

Fig. 21: Relative importance of input parameters

Relative importance of input variables: Learning algorithms such as the back propagation neural network do not give information on the impact of each input parameter or influencing variable upon the predicted output variable. In other words, it is not possible to find out immediately how the weights of the network or the activation values of the hidden neurons are related to the set of data being handled. Instead, ANNs have been presented to the user as a kind of black box whose extremely complex work transforms inputs into predetermined outputs (Montano and Palmer, 2003). To deal with this problem, different interpretative methods for analyzing the effect or importance of input variables on the output of a feedforward neural network have been proposed. These interpretative methods can be divided in two types of methodologies: analysis based on the magnitude of weights and sensitivity analysis (Montano and Palmer, 2003). Analysis based on the magnitude of weights groups together those procedures that are based exclusively on the values stored in the static matrix of weights to determine the relative influence of each input variable on each one of the network outputs (Table 4). On the basis of the magnitudes of weights, the Garson's method (Garson, 1991) was used to determine the relative importance of the input parameters.

As can be seen in Fig. 21, shear modulus is mostly affected by current state of stress (i.e., U_i), aggregate content and with some lower degree by the shear strain amplitude. On the other hand, aggregate size does not have a remarkable effect on the shear modulus. In addition, since pore pressure is closely related to the loading cycles, it can be assumed that the effect of loading cycles on shear modulus has been integrated somehow into the current state of stress.

As shown in Fig. 21, damping ratio is mostly affected by the aggregate content and shear strain amplitude and less by the other parameters. This is in accordance with the results of laboratory tests, showing damping ratio is not affected considerably by loading cycles (Fig. 10, 11), initial confining stress (Fig. 16) and aggregate size (Fig. 17b). It is also interesting to note that pore pressure in aggregate-clay mixtures is mostly affected by aggregate content and initial confining stress and less by the current state of stress and shear strain amplitude. In consistent with the results shown in Fig. 17c, Fig. 21 also reveals that the Mean Aggregate Size (Mas) has a negligible impact on the pore pressure.

CONCLUSIONS

An experimental study was performed on the compacted mixtures of gravel-kaolin and sand-kaolin under different initial confining stresses and shear strain amplitudes to investigate the effects of aggregates on the shear modulus, damping ratio and pore pressure during strain-controlled cyclic triaxial loading. Artificial neural networks (ANNs) were also implemented to model shear modulus, damping ratio and pore pressure in the mixtures. The following conclusions may be drawn based on the study:

- Under low shear strain amplitudes, shear modulus increases with aggregate content, however, it is independent of loading cycles. Under high shear strain amplitudes, shear modulus depends on loading cycles and it decreases with loading cycles. In this case, shear modulus increases with aggregate content prior to 10th cycle of loading, however, it is nearly identical in all mixtures passing the cycle 10. In addition, in all mixtures shear modulus increases linearly with initial confining stress
- In all mixtures, the rate of decrease in shear modulus with loading cycles (i.e., degradation index) decreases with aggregate content. This can be attributed to the increase in pore pressure with aggregate content
- An increase in aggregate content would lead to increase in damping ratio. However, in all mixtures, damping ratio is nearly independent of loading cycles and initial confining stress
- Aggregate size does not affect cyclic deformation properties when aggregate content is low. In high aggregate content mixtures, shear modulus and pore pressure slightly decrease and damping ratio increases when aggregate size is increased
- The observations indicate the potential of well-trained neural networks in developing a relatively general model that can predict shear modulus, damping ratio and pore pressure build-up in the aggregate-clay mixtures. Utilizing current state of state as an input parameter assist in better prediction of the cyclic properties, particularly shear modulus and pore pressure
- Sensitivity analysis of ANNs shows that aggregate content is the most important parameter that affects the dynamic deformation properties. In addition, shear modulus, damping ratio and pore pressure are highly affected by the current state of stress, shear strain amplitude and initial confining stress respectively. Aggregate size has negligible effect on the cyclic properties. The results of the sensitivity analysis fairly support the laboratory observations.

ACKNOWLEDGMENTS

The support of the International Institute of Earthquake Engineering and Seismology (IIEES) which made this work possible is gratefully acknowledged.

REFERENCES

Akbulut, S., A.S. Hasiloglu and S. Pamukcu, 2004. Data generation for shear modulus and damping ratio in reinforced sands using adaptive neuro-fuzzy inference system. Soil Dynamics and Earthquake Eng., 24: 805-814.

Baziar, M.H. and Y. Jafarian, 2007. Assessment of liquefaction triggering using strain energy concept and ANN model: Capacity energy. Soil Dynamics and Earthquake Eng., 27: 1056-1072.

Garson, G.D., 1991. Interpreting neural network connection weights. Artificial Intel. Expert, 6: 47-51.

Haykin, S., 1999. Neural networks: A comprehensive foundation. 1st Edn. Prentice-Hall International Inc, New Jersey, ISBN: 0-13-908385-5.

Idriss, I.M., R. Dobry and R.D. Singh, 1978. Nonlinear behavior of soft clays during cyclic loading. J. Geotech. Eng., 104: 1427-1447.

Jafari, M.K. and A. Shafiee, 1998. Dynamic behavior of mixed materials used for core of Karkheh dam. Proceeding of 11th European Conference on Earthquake Engineering, 1998 Paris, France, pp: 1-179.

Jafari, M.K. and A. Shafiee, 2004. Mechanical behavior of compacted composite clays. Can. Geotech. J., 41: 1152-1167.

Ladd, R.S., 1978. Preparing test specimens using undercompaction. Geotech. Testing J., 1: 39-49.

Lee, J.M. and C.D. Shackelford, 2005. Impact of bentonite quality on hydraulic conductivity of geosynthetic clay liners. J. Geotech. Geoenviron. Eng., 131: 64-77.

Lee, S. and D.G. Evangelista, 2006. Earthquake-induced landslide-susceptibility mapping using an artificial neural network. Natl. Hazards Earth Syst. Sci., 6: 687-695.

Matasovic, N. and M. Vucetic, 1992. A pore pressure model for cyclic straining of clay. Soils and Foundations, 32: 156-173.

McCelland, J.L. and D.E. Rumelhart, 1988. Explorations in Parallel Distributed Processing. 1st Edn. The MIT Press, Boston, ISBN: 0262631296.

Montano, J. and A. Palmer, 2003. Numeric sensitivity analysis applied to feedforward neural networks. J. Neural Comput. Applied, 12: 119-125.

Muir Wood, D. and G. Kumar, 2000. Experimental observations of behaviour of heterogeneous soils. Mech. Cohesive-Frictional Mater., 5: 373-398.

Paolucci, R., P. Colli and G. Giacinto, 2000. Assessment of seismic site effects in 2-D alluvial valleys using neural networks. Earthquake Spectra, 16: 661-680.

Prakasha, K.S. and V.S. Chandrasekaran, 2005. Behavior of marine sand-clay mixtures under static and cyclic triaxial shear. J. Geotech. Geoenviron. Eng., 131: 213-222.

Shafiee, A., 2008. Permeability of granule-clay mixtures. Eng. Geol., 97: 199-208.

Vallejo, L.E. and R. Mawby, 2000. Porosity influence on the shear strength of granular material-clay mixtures. Eng. Geol., 58: 125-136.

Vucetic, M. and R. Dobry, 1991. Effect of soil plasticity on cyclic response. J. Geotech. Eng., 117: 89-107.

Yin, J.H., 1999. Properties and behavior of Hong Kong marine deposits with different clay contents. Can. Geotech. J., 36: 1085-1095.